J. Phys. B: At. Mol. Opt. Phys. **42** (2009) 225501 (6pp) doi:10.1088/0953-4075/42/22/225501

Probe absorptions in an asymmetric double quantum well

Wen-Xing Yang[1,2], Ai-Xi Chen[3], Ting-Ting Zha[1] and Ray-Kuang Lee[2]

[1] Department of Physics, Southeast University, Nanjing 210096, People's Republic of China
[2] Institute of Photonics Technologies, National Tsing-Hua University, Hsinchu 300, Taiwan, Republic of China
[3] Department of Applied Physics, School of Basic Science, East China Jiaotong University, Nanchang 330013, People's Republic of China

E-mail: wenxingyang@seu.edu.cn

Received 16 June 2009, in final form 5 October 2009
Published 5 November 2009
Online at stacks.iop.org/JPhysB/42/225501

Abstract
We investigate the probe absorption properties in an asymmetric coupled double quantum-well structure for both the transient and steady-state processes. Beyond the rotating-wave approximation, we directly simulate the transient dynamics with the density-matrix equations. The probe absorption is found to be completely eliminated under the condition of two-photon resonance, without requiring the one-photon resonance condition. More interestingly, our results show that the absorption properties can be tuned by changing the tunnelling barrier.

It is well known that the optical dispersive and absorption properties of weak probe fields can be controlled by strong coherently coupled fields under the condition of electromagnetically induced transparency (EIT) [1, 2]. EIT and similar phenomena have been deeply studied in dense atomic gases [1–10] starting from its observation in sodium vapours [11], and disclosing new possibilities for nonlinear optics and quantum information processing. In particular, the suppression of both two- and three-photon absorptions in the four-wave mixing (FWM) and hyper-Raman scattering (HRS) has been analysed and discussed in resonant coherent atomic media [7–9].

Compared with the implementation of EIT in dense atomic gases, it is difficult to realize EIT in solid-state media due to a shorter coherence time constant [1]. Nevertheless, some investigations have shown that it is possible to realize EIT and related phenomena in quantum-well (QW) structures [12–17] and molecular magnets [18]. For example, Sadeghi *et al* [13] showed that EIT may be obtained in an asymmetric QW with appropriate driving fields, provided that the coherence between the intersubbands considered is preserved for a sufficiently long time. So quantum coherence and interference in QW structures have attracted great interest due to their potentially important applications in optoelectronics and solid-state quantum information science. In fact, phenomena such as Autler–Townes splitting [17], gain without inversion [19], modified Rabi oscillations and controlled population transfer [20, 21], largely enhanced second harmonic generation [22], controlled optical bistability [23, 24], ultrafast all-optical switching [25, 26] and other novel phenomena [27–33] have been theoretically studied and experimentally demonstrated through the intersubband transitions (ISBT) of semiconductor QWs.

We take note of the model for an asymmetric semiconductor coupled double quantum well [34], in which the realization of coherent sub-millimetre-wave emission was demonstrated by controlling the quantum interference. Instead of the previous work, in this work we focus on the absorptions of a weak probe field based on the condition of two-photon resonance, and analyse the probe absorption properties for the transient and steady-state processes in such a system. Our results show that the probe absorption can be completely eliminated under the condition of two-photon resonance without requiring the one-photon resonance condition. Different from the three-subband quantum well system [14], the absorption properties in our structure can be tuned by changing the tunnelling barrier.

1. The physical model and equations of motion

Let us consider an asymmetric semiconductor coupled double quantum well structure consisting of ten pairs of a 51-monolayer (145 Å) thick wide well and a 35-monolayer (100 Å) thick narrow well, separated by a $Al_{0.2}Ga_{0.8}As$ buffer

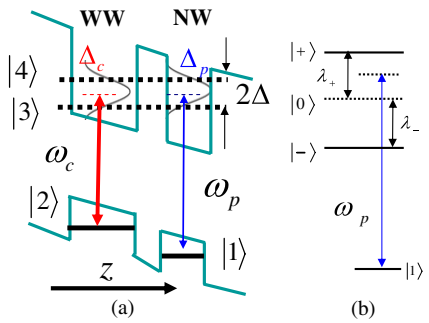

Figure 1. (a) Conduction subband diagram, with a wide well (WW) and a narrow well (NW). A coherent coupling field and another weak probe field have the frequencies ω_c and ω_p, with the detunings Δ_c and Δ_p, respectively. We define one- and two-photon detunings as Δ_p and $\Delta_c - \Delta_p$, respectively. The fields propagate along the growth direction (z axis) with the transverse polarizations. (b) Corresponding dressed-state picture for the case $\Delta_c = 0$, i.e. the three dressed states $|+\rangle$, $|0\rangle$ and $|-\rangle$, respectively.

layer [34], as shown in figure 1. In this coupled QW structure, the first ($n = 1$) electron level in the wide well and that in the narrow well can be energetically aligned with each other by applying a static electric field, while the corresponding $n = 1$ hole bands including heavy holes (hh) and light holes (lh) are never aligned for this polarity of the field. The electrons then delocalize over both wells while the holes remain localized. The subbands E_3 and E_4 of the new bonding ($|3\rangle$) and antibonding ($|4\rangle$) eigenstates of the system are created through the tunnelling, i.e. the coupling effect by the first ($n = 1$) electron levels in the wide well and the narrow well. The energy difference 2Δ of the bonding state and anti-bonding state is determined by the subband splitting, and can be controlled by an electric field applied perpendicular to coupled-quantum wells [35]. Different composites for the narrow and wide wells such as $GaAs/Al_xGa_{1-x}As$, $GaN/Al_xGa_{1-x}N$ and $In_xGa_{1-x}As/AlAs$, can likewise be used here to examine the probe absorption properties at different wavelengths, in which the transition in the ultraviolet or visible regions has very large dipole moment length (10^{-8} m). For more details on the parameters for this system we refer the readers to the literature [36].

As shown in figure 1, the transitions $|2\rangle \leftrightarrow |4\rangle$ and $|2\rangle \leftrightarrow |3\rangle$ are simultaneously driven by a coherent coupling field with the half Rabi frequency $\Omega_c = \mu_{42}E_c/2\hbar$, and a weak probe field is applied to the transitions $|1\rangle \leftrightarrow |4\rangle$ and $|1\rangle \leftrightarrow |3\rangle$ simultaneously with the half Rabi frequency $\Omega_p = \mu_{41}E_p/2\hbar$. E_c and E_p are the amplitudes of the strong-coupling field and the weak probe field, respectively. $\mu_{ij} = \mu_{ij} \cdot \widehat{e}_L$ is the dipole moment for the transition between states $|i\rangle$ and $|j\rangle$ with $\widehat{e}_L$ being the unit polarization vector of the corresponding laser field. As shown in figure 1(a), the probe and the coupling lights propagate along the growth direction (z axis) with the transverse polarization, for coupling a large component of the polarization normal to the layer for the intersubband absorption measurements [31].

In this paper, we focus on the transient and steady-state absorption properties of a weak probe field in our CQW structure. It is well known that treating the transient regime with rotating-wave approximation (RWA) is valid only for the stationary cw driving or slowly varying amplitude driving pulses. In order to examine clearly the absorptions for the transient regime, the interaction Hamiltonian beyond rotating-wave approximation (RWA) can be written as

$$\begin{aligned} H_{\rm int}/\hbar = &-(\Delta_p - \Delta_c)\,|2\rangle\langle 2| - (\Delta + \Delta_p)\,|3\rangle\langle 3| \\ &+ (\Delta - \Delta_p)|4\rangle\langle 4| - [\Omega_c(1 + B^*)|4\rangle\langle 2| \\ &+ k\Omega_c(1 + B^*)\,|3\rangle\langle 2| + \Omega_p(1 + A^*)|4\rangle\langle 1| \\ &+ q\Omega_p(1 + A^*)\,|3\rangle\langle 1| + \text{H.c.}], \end{aligned} \tag{1}$$

with $A = e^{-i2\omega_p t}$, $B = e^{-i2\omega_c t}$. For simplicity of analysis, we have taken $|1\rangle$ as the energy origin. And the corresponding density matrix equations [23]

$$\dot{\rho}_{44} = -\gamma_4\rho_{44} + i\Omega_p(1 + A^*)\rho_{14} + i\Omega_c(1 + B^*)\rho_{24} + \text{c.c.}, \tag{2}$$

$$\dot{\rho}_{33} = -\gamma_3\rho_{33} + iq\Omega_p(1 + A^*)\rho_{13} + ik\Omega_c(1 + B^*)\rho_{23} + \text{c.c.}, \tag{3}$$

$$\begin{aligned} \dot{\rho}_{22} = &-\gamma_2\rho_{22} + \gamma_3\rho_{33} + \gamma_4\rho_{44} + ik\Omega_c(1 + B)\rho_{32} \\ &+ i\Omega_c(1 + B)\rho_{42} + \text{c.c.}, \end{aligned} \tag{4}$$

$$\begin{aligned} \dot{\rho}_{34} = &\,id_{34}\rho_{34} + ik\Omega_c(1 + B^*)\rho_{24} + iq\Omega_p(1 + A^*)\rho_{14} \\ &- i\Omega_c(1 + B)\rho_{32} - i\Omega_p(1 + A)\rho_{31}, \end{aligned} \tag{5}$$

$$\begin{aligned} \dot{\rho}_{24} = &\,id_{24}\rho_{24} + ik\Omega_c(1 + B)\rho_{34} - i\Omega_c(1 + B)(\rho_{22} - \rho_{44}) \\ &- i\Omega_p(1 + A)\rho_{21}, \end{aligned} \tag{6}$$

$$\begin{aligned} \dot{\rho}_{14} = &\,id_{14}\rho_{14} + iq\Omega_p(1 + A)\rho_{34} - i\Omega_p(1 + A)(\rho_{11} - \rho_{44}) \\ &- i\Omega_c(1 + B)\rho_{12}, \end{aligned} \tag{7}$$

$$\begin{aligned} \dot{\rho}_{23} = &\,id_{23}\rho_{23} + i\Omega_c(1 + B)\rho_{43} - ik\Omega_c(1 + B)(\rho_{22} - \rho_{33}) \\ &- iq\Omega_p(1 + A)\rho_{21}, \end{aligned} \tag{8}$$

$$\begin{aligned} \dot{\rho}_{13} = &\,id_{13}\rho_{13} + i\Omega_p(1 + A)\rho_{43} - iq\Omega_p(1 + A)(\rho_{11} - \rho_{33}) \\ &- ik\Omega_c(1 + B)\rho_{12}, \end{aligned} \tag{9}$$

$$\begin{aligned} \dot{\rho}_{12} = &\,id_{12}\rho_{12} + iq\Omega_p(1 + A)\rho_{32} + i\Omega_p(1 + A)\rho_{42} \\ &- ik\Omega_c(1 + B^*)\rho_{13} - i\Omega_c(1 + B^*)\rho_{14}, \end{aligned} \tag{10}$$

together with $\rho_{ij} = \rho_{ji}^*$ and the carrier conservation condition $\rho_{11} + \rho_{22} + \rho_{33} + \rho_{44} = 1$. Here the parameters $k = \mu_{32}/\mu_{42}$ and $q = \mu_{31}/\mu_{41}$ represent the ratios between the dipole moments of the subband transitions, and $d_{34} = 2\Delta + i\gamma_{34}$, $d_{24} = \Delta - \Delta_c + i\gamma_{24}$, $d_{14} = \Delta - \Delta_p + i\gamma_{14}$, $d_{23} = -\Delta - \Delta_c + i\gamma_{23}$, $d_{13} = -\Delta_p - \Delta + i\gamma_{13}$, $d_{12} = \Delta_c - \Delta_p + i\gamma_{12}$. $\Delta = (\omega_{41} - \omega_{31})/2$, $\omega_{31} = \omega_p + \Delta_p - \Delta$, $\omega_{41} = \omega_p + \Delta_p + \Delta$ and $\omega_{21} = \omega_p + \Delta_p - \omega_c - \Delta_c$, where 2Δ represents the frequency splitting between states $|4\rangle$ and $|3\rangle$; ω_{31}, ω_{41} and ω_{21} are subbands splitting between the states $|1\rangle$ and $|3\rangle$, states $|1\rangle$ and $|4\rangle$, and states $|2\rangle$ and $|3\rangle$, respectively; Δ_p and Δ_c denote the probe and coupling field detunings (we define one- and two-photon detunings as Δ_p and $\Delta_c - \Delta_p$, respectively). The population scattering rates γ_i are primarily due to the longitudinal optical phonon emission events at low temperature. The total dephasing rates γ_{ij} ($i \neq j$) are given by $\gamma_{12} = (\gamma_{12}^{\rm dph} + \gamma_2)/2$, $\gamma_{13} = (\gamma_{13}^{\rm dph} + \gamma_3)/2$, $\gamma_{14} = (\gamma_{14}^{\rm dph} + \gamma_4)/2$,

$\gamma_{23} = (\gamma_{23}^{\rm dph} + \gamma_2 + \gamma_3)/2$, $\gamma_{24} = (\gamma_{24}^{\rm dph} + \gamma_2 + \gamma_4)/2$ and $\gamma_{34} = (\gamma_{34}^{\rm dph} + \gamma_3 + \gamma_4)/2$ [23], where the pure dipole dephasing $\gamma_{ij}^{\rm dph}$ are assumed to be a combination of quasi-elastic interface roughness scattering and acoustic phonon scattering [17]. It should be noted that the electron sheet density of the quantum well structure considered here is small such that additional broadenings induced by the carrier–carrier effect have very small influence on our results [13, 37], and the additional broadening can be readily included by first deriving the motion equations (2)–(10). A more complete theoretical treatment [38] for the dephasing rates should involve incorporation of the decay mechanisms into the Hamiltonian of the system. Here we have adopted the phenomenological approach of treating the decay mechanisms, which has proven to be well studied for modelling quantitatively experimental results [31]. Besides, we should address that the model can only be applied to direct band-gap semiconductors and also for cases (such as AlGaAs structures) in which there is low mass dispersion in the conduction subbands as given by Kane's model [12].

Due to the states $|3\rangle$ and $|4\rangle$ being bonding and antibonding states, we can take $k = -q = 1$ ($\mu_{31} = \mu_{41} = \mu_p$, $\mu_{32} = \mu_{42} = \mu_c$) to simplify our numerical calculations. Besides, we take $\gamma_{12} = 0$ according to [39]. In the limit of a weak probe, the absorption coefficient for the probe field is governed by the imaginary part of the time-dependent polarization $P(t) = \mu_p[\rho_{31}(t) + \rho_{41}(t)]$. In the following sections, we will directly examine the transient absorption of the weak probe field by numerically integrating equations (2)–(10) with a given initial condition. Our analysis is valid to examine the transient-state absorption by using $\mathrm{Im}[\rho_{31}(t) + \rho_{41}(t)]$ as long as ω_p is much larger than the decay rates. With the initial conditions $\rho_{11}(0) = 1$, $\rho_{22,33,44}(0) = 0$ and $\rho_{ij}(0) = 0$ for $i \neq j$ ($i, j = 1, 2, 3, 4$), we solve the time-dependent equations (2)–(10) by a standard fourth-order Runge–Kutta method, with the integration time (γt) step 0.05. Note that, in this paper, the parameters $\Omega_{c,p}$, $\Delta_{c,p}$, γ_i, γ_{ij} and Δ are set in units of constant γ ($\gamma = 2\gamma_{34}$) in our numerical simulations.

2. The probe absorption for the transient process

In figure 2, we show the time evolution of the absorption coefficient under the resonance condition $\Delta_c = \Delta_p = 0$ with the parameters $\omega_p = 16\gamma$, $\omega_c = 12\gamma$, $\Omega_p = 0.01\gamma$, $\Omega_c = 3\gamma$, $\gamma_3 = \gamma_4 = 0.4\gamma$ and $\gamma_{ij}^{\rm dph} = 0.2\gamma$. By decreasing Δ, the corresponding oscillatory frequency decreases, but the oscillatory amplitude increases. The probe field shows the same oscillatory curve versus the time before reaching its steady state, with similar periodic absorption and amplification behaviour as in high density atomic systems. Initially the probe absorption increases rapidly to a maximum peak value, then it decreases gradually and again oscillates to a steady-state value. In the atomic system, the transient behaviour of the probe field is strongly dependent on the external coherent coupling field, and the oscillatory frequency is determined by the Rabi frequency of the coherent coupling field. The superiority of our four-subband model

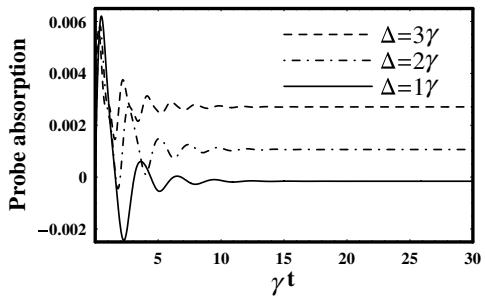

Figure 2. Numerical simulation for time evolution of the probe absorption with different splitting Δ under the resonant condition $\Delta_p = \Delta_c = 0$. Other simulation parameters used are $\omega_p = 16\gamma$, $\omega_c = 12\gamma$, $\Omega_p = 0.01\gamma$, $\Omega_c = 3\gamma$, $\gamma_3 = \gamma_4 = 0.4\gamma$ and $\gamma_{ij}^{\rm dph} = 0.2\gamma$.

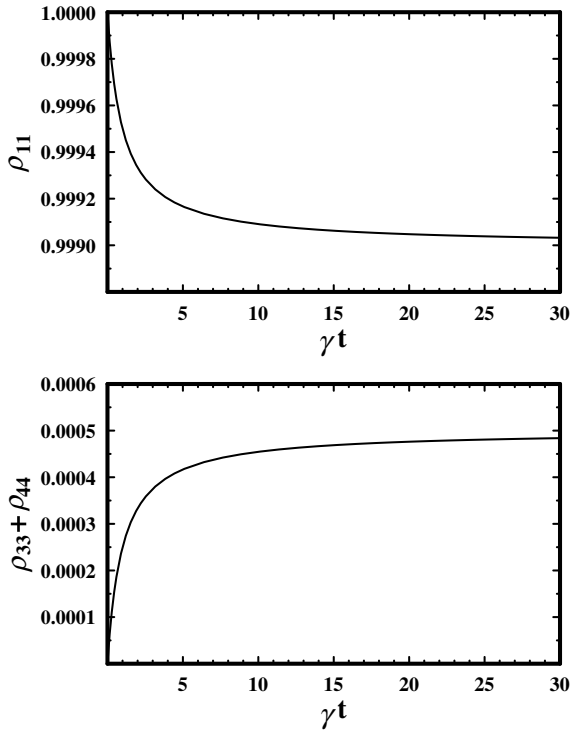

Figure 3. Numerical simulation for time evolution of the population distribution ρ_{11} and $\rho_{33} + \rho_{44}$ with $\Delta = 3\gamma$. Other parameters used are the same as those in figure 2.

in QW structures compared with the atomic system can be obviously seen, namely the transient behaviour of the probe field can be tuned by changing the frequency splitting 2Δ through adjusting the tunnelling barrier, as illustrated in figure 2. In figure 3, we give the time evolution of the populations ρ_{11} and $\rho_{33} + \rho_{44}$. From figure 3, one can find that almost all particles are trapped in the ground state $|1\rangle$.

For our coupled QW structure, when the subband splitting between the two upper states vanishes, $\Delta = 0$, our model can be reduced to a standard Λ-configuration three-subband system (TSS) (such as the three subbands $|1\rangle$, $|2\rangle$ and $|3\rangle$) [14]. Thus, we can briefly compare our results with the corresponding TSS. We show in figure 4 the transient absorption of the probe field versus the probe dimensionless

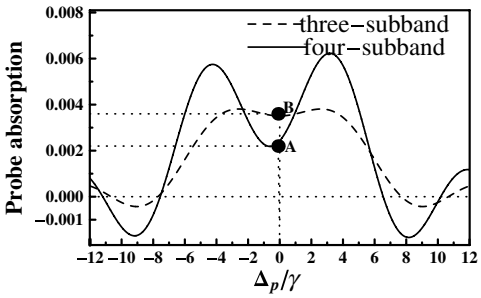

Figure 4. The transient absorptions of the probe field as a function of the dimensionless probe detuning Δ_p/γ at the time $t = 2/\gamma$ with $\Omega_p = 0.01\gamma$ and $\Delta_c = 0$, where $\Delta = \gamma$ and $\Delta = 0$ correspond to four-subband and three-subband systems, respectively. Other parameters used are the same as those in figure 2.

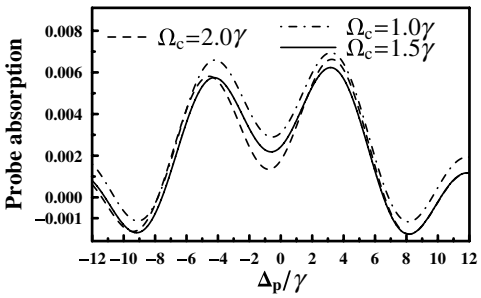

Figure 5. The transient absorptions of the probe field as a function of the dimensionless detuning Δ_p/γ by choosing $t = 2/\gamma$, $\Delta_c = 0$ and $\Delta = \gamma$ with different coherent coupling fields. Other simulation parameters used are the same as those in figure 2.

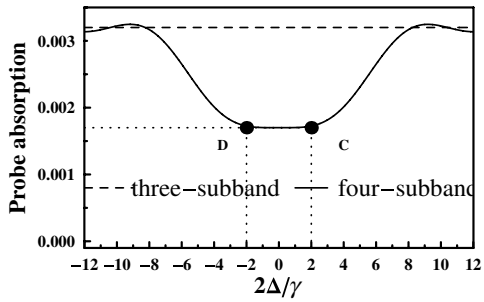

Figure 6. The transient absorptions of the probe field as a function of the dimensionless splitting $2\Delta/\gamma$ at the time $t = 2/\gamma$ with $\Delta_p = \Delta_c = 0$ and $\Delta = \gamma$. Other simulation parameters used here are the same as those in figure 2.

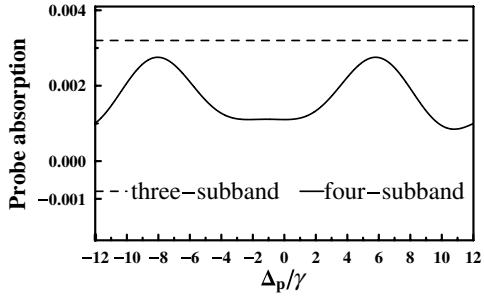

Figure 7. The transient absorptions of the probe field as a function of the dimensionless probe detuning Δ_p/γ at the time $t = 2/\gamma$ with $\Delta = \gamma$ under the two-photon resonance condition $\Delta_c = \Delta_p$. Other simulation parameters used here are the same as those in figure 2.

detuning Δ_p/γ. At the centre of the probe detuning, $\Delta_p = 0$, the magnitude of the transient absorption, marked as A, is much smaller than that for a standard TSS, marked as B. With the appropriate values of the parameters we show in figure 5 the transient absorption spectra for a four-subband coupled QW structure for different intensities of the coupling field Ω_c. From figure 5, one can find that the notch in the absorption spectra becomes deep accordingly as the value of Ω_c increases, as expected for the coherent EIT process. At the same time, the transparency width becomes more pronounced as the Rabi frequency of the coherent coupling field increases. From the above analysis, we can conclude that the transient absorption of the probe field at the centre of the detuning in our four-subband coupled QW model, $\Delta_p = 0$, can be considerably suppressed and much smaller than the corresponding TSS.

The transient absorption for such a weak probe laser versus the subband splitting, 2Δ, is shown in figure 6, in which the dashed line describes the magnitude of the probe absorption coefficient for a standard TLS under the condition $\Delta_p = \Delta_c = 0$, while the solid curve describes our four-subband system, in which the line CD corresponds to the minima of the probe absorption. We observe that the magnitude of the transient absorption coefficient for the probe field is always smaller than that in a TSS. As shown in figure 7, we plot the absorption profiles versus the dimensionless probe detuning Δ_p under the two-photon resonance condition, i.e. $\Delta_p = \Delta_c$. For this case, we also find that the maximal absorption peak is always smaller than that in a standard TLS.

3. The probe absorption under the steady-state condition

Based on the above transient-state analysis, the initial populations are in the ground state $|1\rangle$, i.e. $\rho_{11} \simeq 1$ and $\rho_{22} \simeq \rho_{33} \simeq \rho_{44} = 0$. Under the rotating-wave approximation and the steady-state condition ($\partial\rho_{ij}/\partial t = 0$), the general steady-state solutions for equations (2)–(10) can be derived analytically. Then under the perturbation expansion $\rho_{ij} = \sum_k \rho_{ij}^{(k)}$, where $\rho_{ij}^{(k)}$ is the kth-order part of ρ_{ij} in terms of Ω_p, it can be shown that $\rho_{ij}^{(0)} = 0$ $(i \neq j)$ and $\rho_{22}^{(k)} = \rho_{33}^{(k)} = \rho_{44}^{(k)} = 0$. We can readily obtain

$$\rho_{12}^{(1)} = \frac{\mathrm{i}kqd_3\Omega_c\Omega_p^*}{D}, \qquad \rho_{13}^{(1)} = \frac{(\mathrm{i}qd_3d_1 + \mathrm{i}q|\Omega_c|^2)\Omega_p^*}{D},$$
$$\rho_{14}^{(1)} = -\frac{\mathrm{i}kq|\Omega|^2\Omega_p^*}{D}, \tag{11}$$

where $D = \mathrm{i}d_2|\Omega_c|^2 + \mathrm{i}d_3(d_2d_1 - k^2|\Omega_c|^2)$ with $d_1 = \Delta_c - \Delta_p + \mathrm{i}\gamma_{12}$, $d_2 = -\Delta_p - \Delta + \mathrm{i}\gamma_{13}$ and $d_3 = \Delta - \Delta_p + \mathrm{i}\gamma_{14}$. From equation (11), one can also find the tedious and intricate expressions for the solutions, but without a clear physical insight. So we perform the numerical calculation here, as shown in figures 8 and 9. The present result is most clearly understood according to the dressed states produced by the strong coupling field ω_c as shown in figure 1(b), i.e. the transitions $|2\rangle \leftrightarrow |3\rangle$ and $|2\rangle \leftrightarrow |4\rangle$ together with the coupling field treated as a total system forming the dressed states (this standard method has been described in [40] and [26] can also

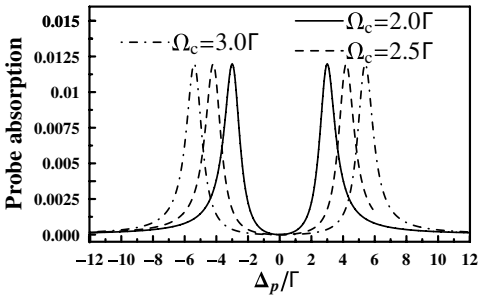

Figure 8. Imaginary part of the susceptibility for the probe field as a function of the dimensionless detuning Δ_p/γ with $\Delta = \gamma$ and $\Delta_c = 0$ under the steady-state condition. Other parameters used here are the same as those in figure 2.

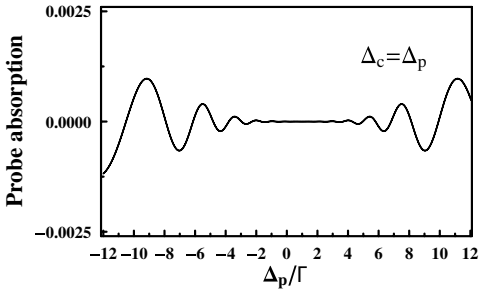

Figure 9. Imaginary part of the susceptibility for the probe field as a function of the dimensionless detuning Δ_p/γ with $\Delta = \gamma$ under the condition of two-photon resonance in a steady-state regime. Other parameters are the same as in figure 2.

be referred to for the semiconductor QW structures). Under the action of the coherent coupling field, the two upper states could be split into three dressed states $|\pm\rangle$ and $|0\rangle$. The eigenstates of the dressed states for the case $\Delta_c = 0$ can be given by

$$|+\rangle = -\frac{\Omega_c}{B}|2\rangle - \frac{1}{2}\frac{\Delta - B}{B}|3\rangle + \frac{1}{2}\frac{\Delta + B}{B}|4\rangle, \tag{12}$$

$$|0\rangle = \frac{\Delta}{B}|2\rangle - \frac{\Omega_c}{B}|3\rangle + \frac{\Omega_c}{B}|4\rangle, \tag{13}$$

$$|-\rangle = \frac{\Omega_c}{B}|2\rangle + \frac{1}{2}\frac{\Delta + B}{B}|3\rangle - \frac{1}{2}\frac{\Delta - B}{B}|4\rangle, \tag{14}$$

with $B = \sqrt{\Delta^2 + 2\Omega_c^2}$. The corresponding eigenvalues are given by $\lambda_0 = 0$ and $\lambda_\pm = \pm\sqrt{\Delta^2 + 2\Omega_c^2}$ and the dressed-state transition dipole moments can be derived as $\mu_{+1} = \langle +| P |1\rangle = \mu_p$, $\mu_{01} = \langle 0| P |1\rangle = 0$ and $\mu_{-1} = \langle -| P |1\rangle = \mu_p$, where $P = \mu_p(|3\rangle\langle 1| + |4\rangle\langle 1|)$ represents the polarization operator of the probe transition.

Based on the above analysis, it is straightforward to show that the transition between dressed states $|0\rangle$ and $|1\rangle$ is forbidden due to the couplings of $|1\rangle \leftrightarrow |3\rangle$ and $|1\rangle \leftrightarrow |4\rangle$. We can observe in figure 8 two symmetric absorption peaks with the same amplitude on the probe spectra in the case of $\Delta_c = 0$ because of the relation $\mu_{+1} = \mu_{-1}$. The two absorption peaks correspond respectively to the dressed-state transitions $|1\rangle \leftrightarrow |+\rangle$ and $|1\rangle \leftrightarrow |-\rangle$, so the peaks are always located at $\Delta_p = \pm\sqrt{\Delta^2 + 2\Omega_c^2}$, and the difference between them becomes large as Ω_c increases. Since the transition $|1\rangle \leftrightarrow |0\rangle$ in the dressed-state picture is cancelled out by the interference and this interference always makes a negative contribution to the probe absorption, thus it can be understood that the probe absorption at the centre can be completely suppressed as expected. As shown in figure 9, we plot the probe absorption profile versus the probe detuning Δ_p. One can find that the probe absorption spectra are always approximately equal to zero within a wide range of the splitting frequency 2Δ. This means that if the two-photon resonance is satisfied, we can observe the transparency window without requiring the condition that one- or two-photon detuning exactly vanishes.

4. Discussions and conclusion

In the present study, we only focus on the condition of low temperatures up to 10 K, and have neglected other many-body effects such as the depolarization effect, which renormalizes the free-carrier and carrier-field contributions. These contributions and their interplay have been investigated quite thoroughly in the literature [38, 41, 42]. Note that, due to the small carrier density considered here, these effects only give a small correction.

In conclusion, we have analysed the probe absorption properties in a coupled QW for the transient process by directly integrating the density matrix equations (2)–(10) beyond the RWA. In the transient-state regime, the magnitude of the probe absorption at the centre of the probe detunings, $\Delta_p = 0$, can be greatly suppressed. Compared with the EIT scheme in the TSS system [14] (corresponding to $\Delta = 0$ in our coupled QW structure), our results show that the transparency window is much broader due to the existence of the tunnel-coupling splitting 2Δ. Besides, we do not require the condition that one-photon detuning (Δ_p) or two-photon detuning ($\Delta_c - \Delta_p$) is exactly zero. In addition, we also numerically and analytically show the probe absorption mechanism for the steady-state process under the RWA. In the steady-state process, the probe absorption can be largely suppressed with the coupling field resonance, $\Delta_c = 0$, and eliminated completely under the condition of two-photon resonance, $\Delta_p = \Delta_c$. As a result, the present investigation may provide the possibility for obtaining transparency in solids by using an asymmetric coupled QW structure. Our calculations also provide a guideline for the optimal design to achieve very fast and low-threshold all-optical switches in such semiconductor systems which are much more practical than those in atomic systems due to their flexibility.

Acknowledgments

The research is supported in part by NSFC under grant nos 10704017 and 10874050, by NFRPC under grant nos 2007CB936300 and 2005CB724508. We would like to thank Ite Yu for his enlightening discussions.

References

[1] Harris S E 1997 *Phys. Today* **50** 36
[2] Fleishhauer M, Imamoglu A and Marangos J P 2005 *Rev. Mod. Phys.* **77** 633
[3] Arimondo E 1996 *Progress in Optics* ed E Wolf (Amsterdam: Elsevier)
[4] Hau L V *et al* 1999 *Nature* **397** 594
Liu C *et al* 2001 *Nature* **409** 490
[5] Agarwal G S and Harshawardhan W 1996 *Phys. Rev. Lett.* **77** 1039
[6] Wu Y and Yang X 2007 *Phys. Rev. Lett.* **98** 013601
[7] Wu Y and Yang X 2000 *Phys. Rev.* A **62** 013603
Yang X and Wu Y 2006 *J. Phys. B: At. Mol. Opt. Phys.* **39** 2285
[8] Wu J H *et al* 2003 *Opt. Lett.* **28** 654
Wu Y 2005 *Phys. Rev.* A **71** 053820
[9] Harris S E and Yamamoto Y 1998 *Phys. Rev. Lett.* **81** 3611
[10] Wu Y, Saldana J and Zhu Y 2003 *Phys. Rev.* A **67** 013811
[11] Alzetta G *et al* 1976 *Nuovo Cimento* B **36** 5
[12] Nikonov D E, Imamoglu A and Scully M O 1999 *Phys. Rev.* B **59** 12212
[13] Sadeghi S M, Leffler S R and Meyer J 1999 *Phys. Rev.* B **59** 15388
[14] Silvestri L *et al* 2002 *Eur. Phys. J.* B **27** 89
Phillips C C *et al* 2000 *Physica* E **7** 166
[15] Ginzburg P and Orenstein M 2006 *Opt. Express* **14** 12467
[16] Serapiglia G B *et al* 2000 *Phys. Rev. Lett.* **84** 1019
[17] Dynes J F *et al* 2004 *Phys. Rev. Lett.* **94** 157403
[18] Wu Y and Yang X 2007 *Appl. Phys. Lett.* **91** 094104
[19] Imamoglu A and Ram R J 1994 *Opt. Lett.* **19** 1744
[20] Bastista A A and Citrin D S 2004 *Phys. Rev. Lett.* **92** 127404
[21] Paspalakis E, Tsaousidou M and Terzis A F 2006 *Phys. Rev.* B **73** 125344
[22] Tsang L, Ahn D and Chuang S L 1988 *Appl. Phys. Lett.* **52** 697
[23] Stockman M I, Pandey L N, Muratov L S and George T F 1993 *Phys. Rev.* B **48** 10966
[24] Joshi A and Xiao M 2004 *Appl. Phys.* B **79** 65
Wijewardane H O and Ullrich C A 2004 *Appl. Phys. Lett.* **84** 3984
[25] Schmidt H and Ram R J 2000 *Appl. Phys. Lett.* **76** 3173
[26] Wu J H *et al* 2005 *Phys. Rev. Lett.* **95** 057401
[27] Dynes J F and Paspalakis E 2006 *Phys. Rev.* B **73** 233305
[28] Faist J *et al* 1997 *Nature* **390** 589
[29] Sadeghi S M *et al* 2000 *Phys. Rev.* B **62** 15386
[30] Paspalakis E *et al* 2007 *Proc. SPIE* **6582** 65821N
[31] Liu H C and Capasso F 2000 *Intersubband Transitions in Quantum Wells: Physics and Devices Applications* (San Diego: Academic)
[32] Heyman J N *et al* 1994 *Phys. Rev. Lett.* **72** 2183
Craig K *et al* 1996 *Phys. Rev. Lett.* **76** 2382
Galdrikian B and Birnir B 1996 *Phys. Rev. Lett.* **76** 3308
Nikonov D E *et al* 1997 *Phys. Rev. Lett.* **79** 4633
[33] Olaya-Castro A *et al* 2003 *Phys. Rev.* B **68** 155305
[34] Roskos H G *et al* 1992 *Phys. Rev. Lett.* **68** 2216
Luo M S C *et al* 1993 *Phys. Rev.* B **48** 11043
Planken P C M *et al* 1993 *Phys. Rev.* B **48** 4903
[35] Raichev O E 1995 *Phys. Rev.* B **51** 17713
[36] Piprek J and Nakamura S 2002 *Proc. IEEE* **149** 145
[37] Waldmüller I *et al* 2004 *Phys. Rev.* B **69** 205307
[38] Haug H 1992 *Phys. Status Solidi (b)* **173** 139
[39] Neogi A *et al* 1999 *Opt. Commun.* **159** 225
[40] Scully M O and Zubairy M S 1997 *Quantum Optics* (New York: Cambridge University Press)
[41] Shih T *et al* 2005 *Phys. Rev.* B **72** 195338
[42] Warburton R J *et al* 1996 *Phys. Rev.* B **53** 7903
Nikonov D E *et al* 1997 *Phys. Rev. Lett.* **79** 4633